Supporting Information

Table of Content

1 Experimental Section

1.1 Synthesis of Gold Nanoparticles

1.1.1 Preparation of the gold nanoparticles (GNP)

GNPs have been synthesized by using a modification of the method reported in literature by Bastús et al.[1] A solution of 2.2 mM sodium citrate in Milli-Q water (150 mL) was heated on oil bath in a 250 mL three-necked round-bottomed flask (equipped with a condenser to avoid solvent evaporation) for 15 min under constant stirring. As soon as the solution started boiling, 1 mL of $HAuCl_4$ (25 mM) was injected. After 10 min, of reaction, resulting particles are ~12 nm in diameter and coated with negatively charged citrate (water soluble). Immediately after Au seed synthesis and without changing the reaction recipient, the dispersion was cooled to 90. 55 mL of the stock solution is removed and 55mL of 60 mM sodium citrate solution is injected followed by two additions of 1mL of 25mM $HAuCl_4$ solution. After 30 min by repeating this process, the desire nanoparticle size, ranging from 10 to 90 nm is obtained.

1.2 Preparation of gold nanoparticles coated with Transferrin protein

The GNP@Tf NPs were prepared fresh before each experiment. 70, 50, and 20 nm GNP were incubated with 1.25mg of Tf (16nmol) in 0.5mL with a final concentration of 5e10 np/mL. After 1 h incubation at RT at constant agitation, NPs were washed two times with MES and two times with PBS by centrifugation at 10000 rpm for 5 mins (10 mins for 20nm GNPs). The NP concentration was determined by NTA before and after the purification steps necessaries to remove the unbound Tf protein.

1.3 Core-shell model

A simple model to analyze data for shell-coated particles was developed to get an estimation of the shell thickness as it is described in [4]. If a spherical particle, composed of an inorganic core of density ρ_c, with a diameter D_c, and a shell of density ρ_s, and thickness D_s, is placed in a rotating disc filled with a fluid of density ρ_f, the particle will suffer a drag force of the form:

$$Fd = 3\pi D_s \eta v \qquad (1)$$

where D_s (D_c+2δ) is the total diameter of the core-shell particle, η is the viscosity of the fluid and v is the settling velocity of the particle. This force will be balanced by the centrifugal force:

$$Fc = m\omega^2 R \qquad (2)$$

where R is the distance from the particle to the axis of rotation, m is the particle mass and ω is the angular velocity of the disc (and the particle within). Considering the buoyancy and the presence of two different materials in the particle, the mass m can be written as:

$$m=\frac{\pi}{6}(\rho_c D_c^3+\rho_s(D_s^3-D_c^3)-\rho_f D_s^3) \qquad (3)$$

At equilibrium between these forces, we have:

$$(\rho_c-\rho_s)\frac{D_c^3}{D_s}+(\rho_s-\rho_f)D_s^2=\frac{18\eta 1 dR}{\omega^2 R dt} \qquad (4a)$$

Solving this equation for the simplest case where there is no physical shell (ρs= ρc), we obtain:

$$[(\rho_c - \rho_s)D^2]\cdot t = \frac{18\eta}{\omega^2}\ln\left(\frac{R_f}{R_0}\right) \quad (4b)$$

where dR/dt is the radial velocity, t is the time elapsed while the particle moves between the initial R_0 and the final R_f position and D is the measured diameter. Since all DCS measurements are calibrated for this equation in the presence of a shell one can extract a real particle diameter Ds, from the measured D using the following equation:

$$\frac{(\rho_c - \rho_s)D_c^3}{(\rho_c - \rho_f)D_s} + \frac{(\rho_s - \rho_f)}{(\rho_c - \rho_f)}D_s^2 = D^2 \quad (5)$$

Generally, from the apparent measured diameter of these peaks we extracted the shell thickness, δ, by knowing ρ_c, ρ_f, ρ_s and D_c. In particular, D_c is set to the value obtained for the bare gold or polystyrene NPs in buffer and ρ_c is the density of the material (1.04 g/cm^3 for polystyrene NP and 19 g/cm^3 for gold NP). Actually, ρ_f should be considered as a function of the radius R but it is substituted with an effective quantity, which is its mean value between R_0 and R_f. In our case, a source of uncertainty for the quantitative determination of the shell thickness is the choice for the shell density since we do not have experimental values for the hydration degree and the actual conformation of the adsorbed proteins. The established mean density value for hydrated protein crystals is 1.23 g/cm^3.

2 Supplementary Figures

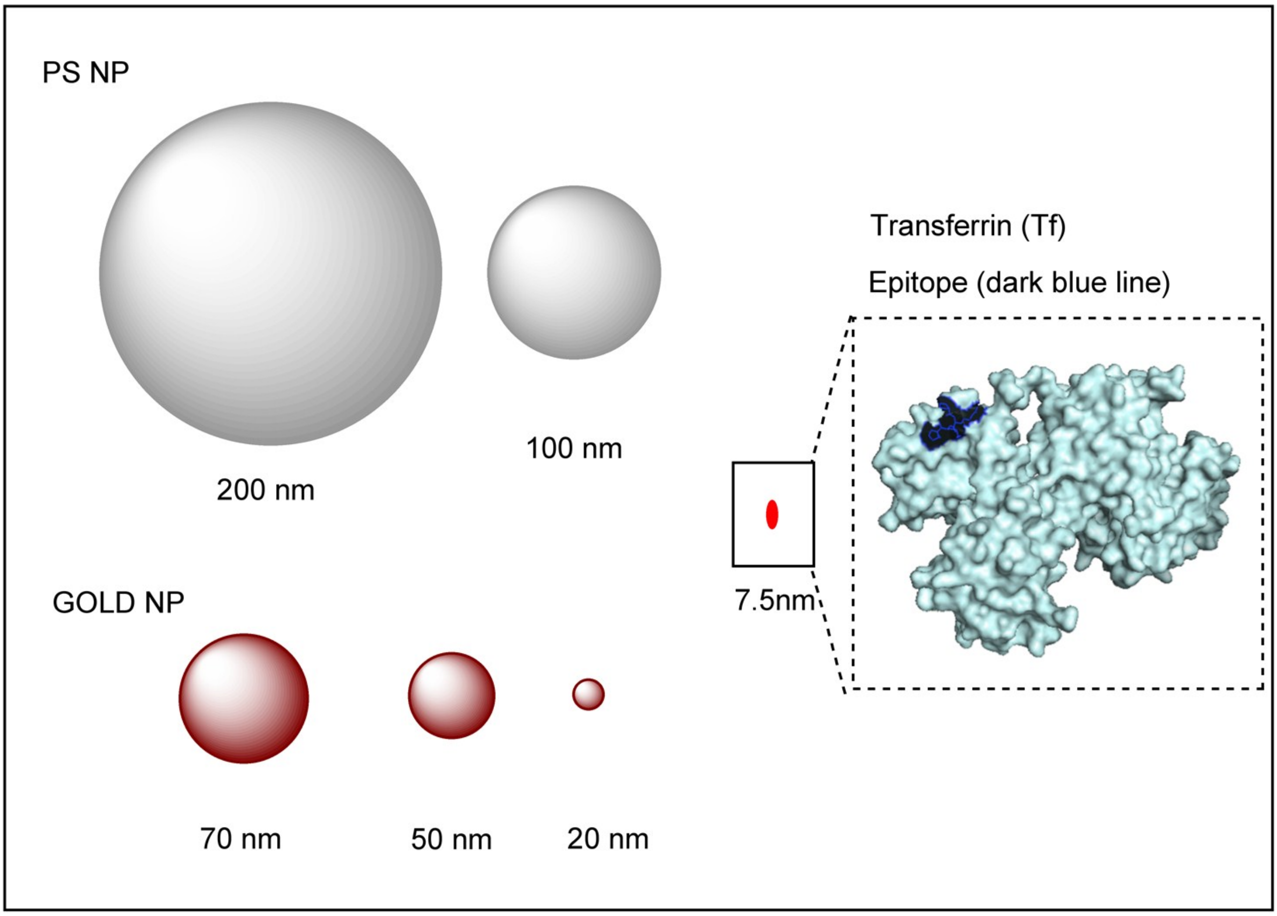

Scheme 1. Transferrin structure by PyMOL®. Monoclonal antibody anti-Tf (mAb-Tf) binding site: aa 142-145. PS and gold NPs of different sizes were employed.

sample	DCS (nm) NP	DCS (nm) NPTf	PDI NP	Z-Av (nm) NP	Int (nm) NP	PDI NPTf	Z-Av (nm) NPTf	Int. (nm) NPTf	NTA (nm) NPTf	NTA (np/mL) NPTf
200-PSSO3	225.9	274.6	0.023	241	249	0.022	259	271	222.2(9)	$6.9e^{11} \pm 1.4e^{11}$
200-PSCOOH	182.3	203.5	0.02	170	177	0.028	184	192	177,8(3)	$5.1e^{11} \pm 6.3e^{10}$
100-PSSO3	107	130	0.027	98	103	0.023	118	123		$8.2e^{11} \pm 1e^{11}$
100-PSCOOH	98	146	0.021	74	77	0.12	122	138		$1e^{12} \pm 8e^{10}$

Table S1. PSNP and PSNP@Tf characterization by DCS, DLS and NTA.

Sample	DCS (nm) NP	DCS (nm) NPTf	PDI	Z-Av (nm)	Int (nm)	NTA (nm) NPTf	NTA (np/mL) NPTf
70-GNPCit	69	70.2	0.095	80	90	86.7	$4.8e^{10}$
50-GNPCit	50	46.2	0.16	60	71	65	$3.8e^{10}$
20-GNPCit	23.15	20.7	0.25	29	35	33	$6.6e^{10}$

Table S2. GNP and GNP@Tf characterization by DCS, DLS and NTA.

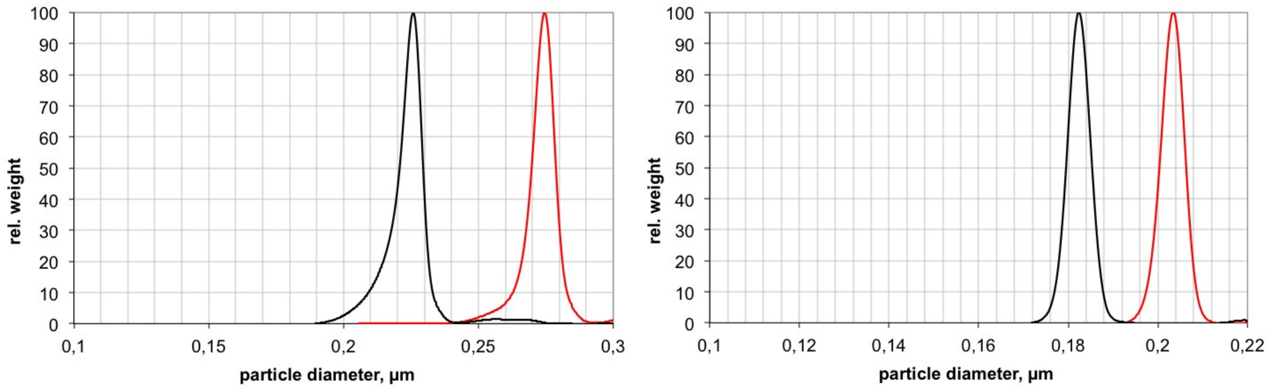

Figure S1. Graphs DCS (NP black line and NP@Tf red line): a) 200 nm PS SO_3 NP b) 200 nm PS COOH NP.

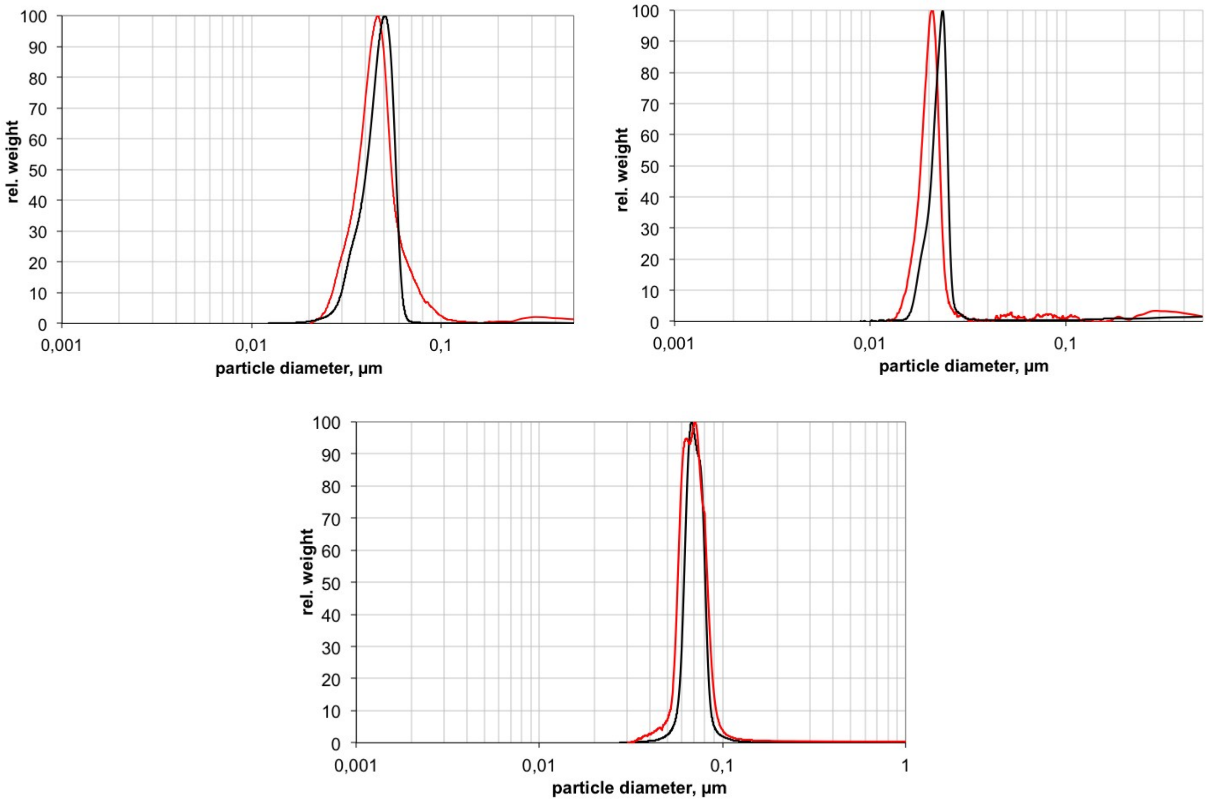

Figure S2. Graphs DCS (NP black line and NP@Tf red line): a) 20 nm GNP Citrate, b), 50 nm GNP Citrate, c) 70 nm GNP Citrate.

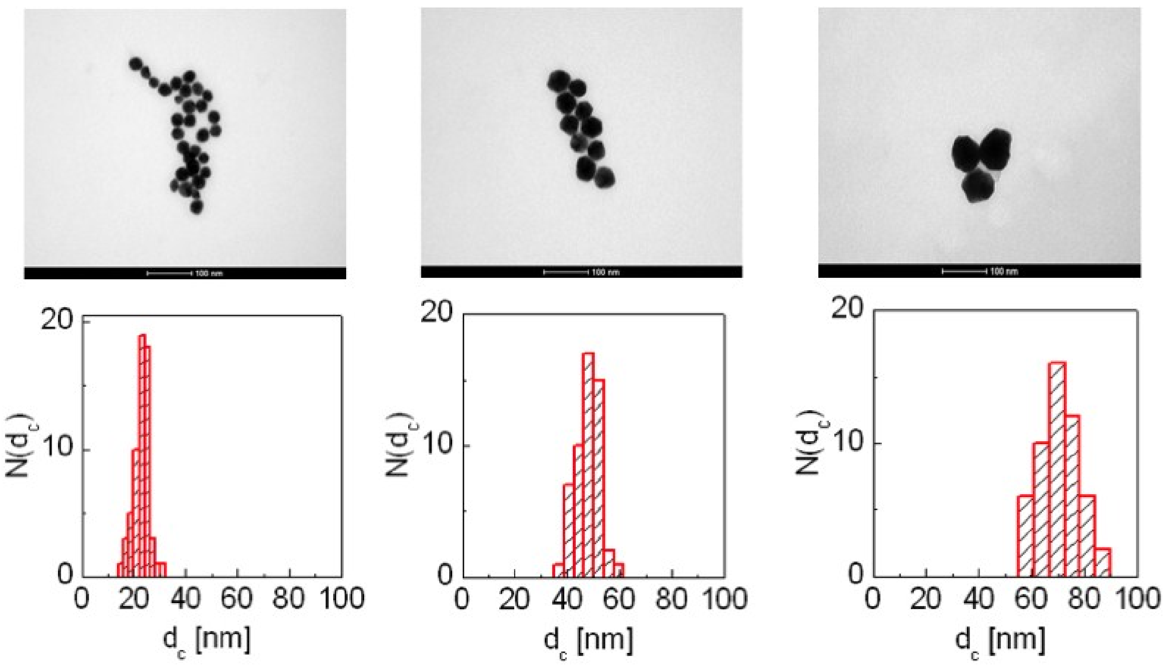

Figure S3. TEM micrographs and statistical size distribution of GNPs: 20 nm GNP Citrate, 50 nm GNP Citrate and 70 nm GNP Citrate (scale bar: 100 nm).

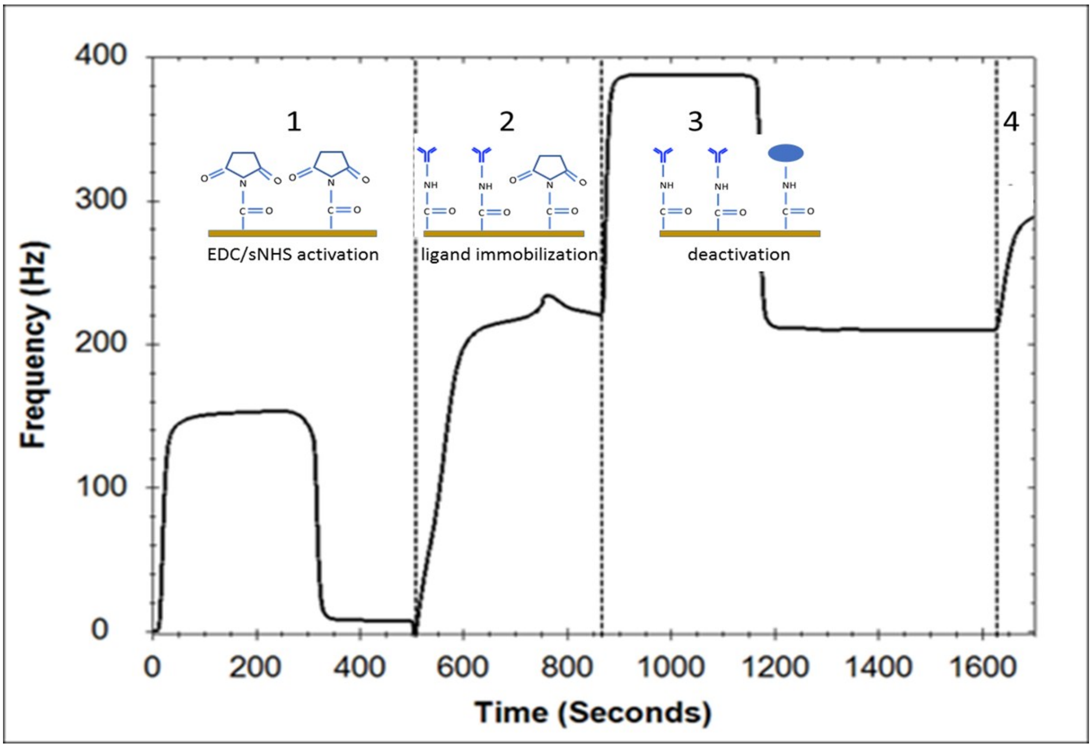

Figure S4. Data for QCM Ab functionalization. Sensorgram showing: 1) activation of surface with EDC/sNHS, 2) immobilization of the ligand; monoclonal antibody anti-Tf (mAb-Tf) at a concentration of 50 µg/mL, 3) deactivation with ethanolamine (EA), 4) injection of NP solution.

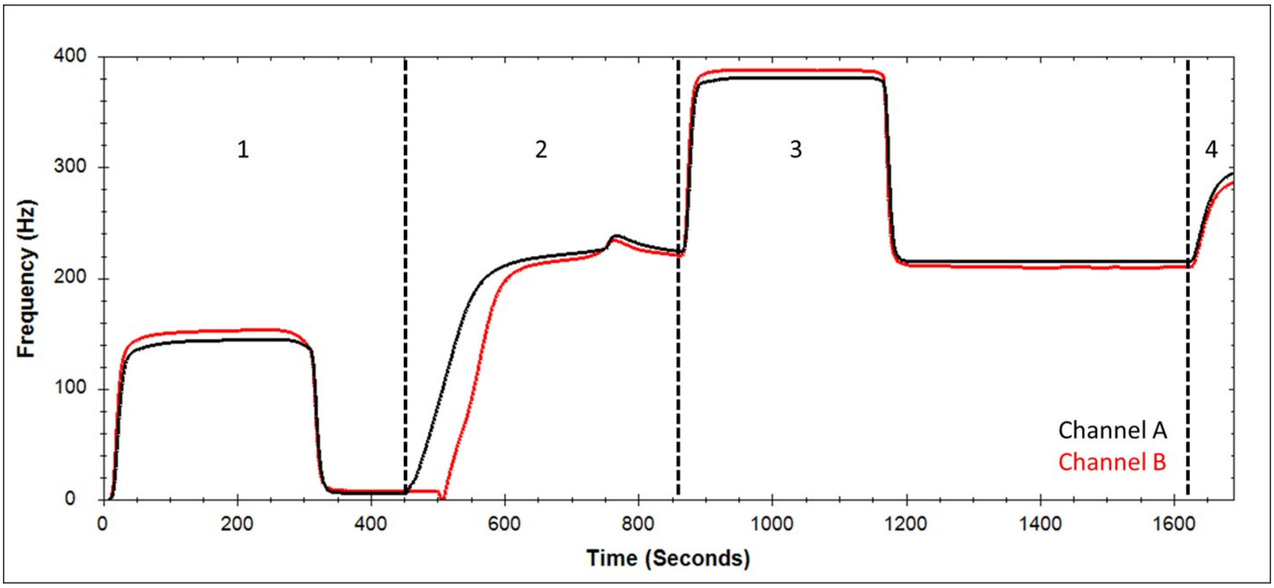

Figure S5. Sensorgram showing: 1) activation of surfaces with EDC/sNHS, 2. successful immobilization of the ligand; mAb-Tf at a concentration of 50 µg/mL, 3. deactivation with ethanolamine (EA), 4. injection of NP solution.

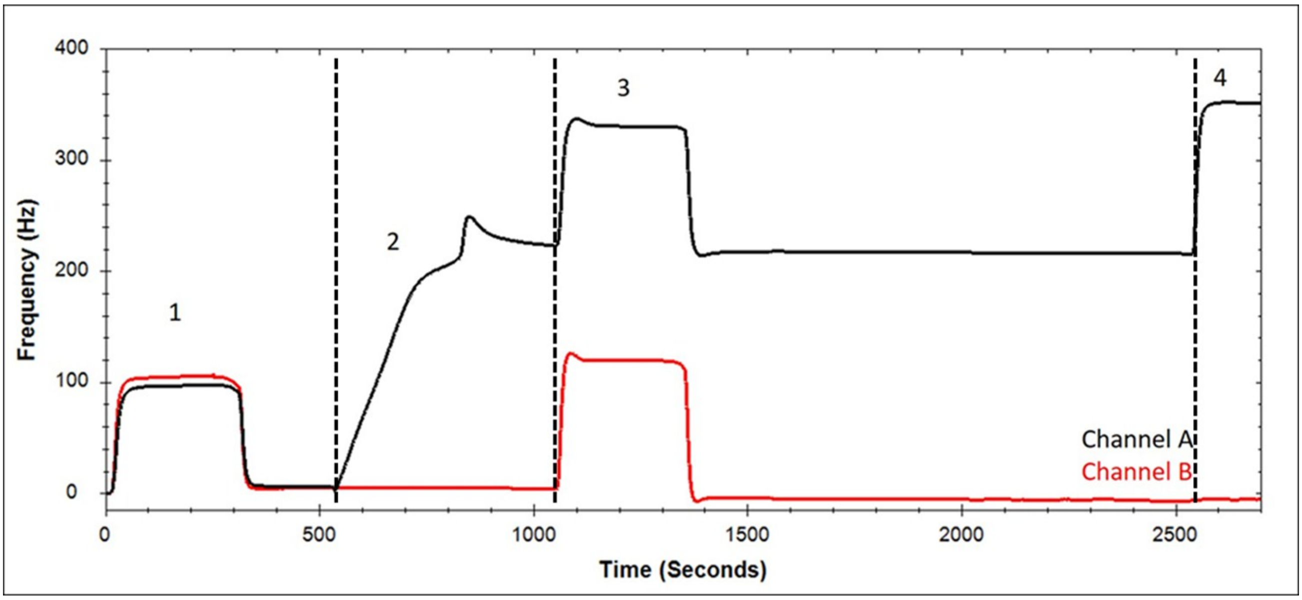

Figure S6. Sensorgram showing the different steps of immobilization of the ligand (mAb-Tf) and binding to the analyte (Tf): 1) activation with EDC/sNHS, 2) mAb-Tf immobilization, 3) deactivation with ethanolamine (EA), 4) Tf injection at a concentration of 50 µg/mL. Channel A: LNB surface with mAb-Tf (amine coupling), Channel B: activated/deactivated LNB surface.

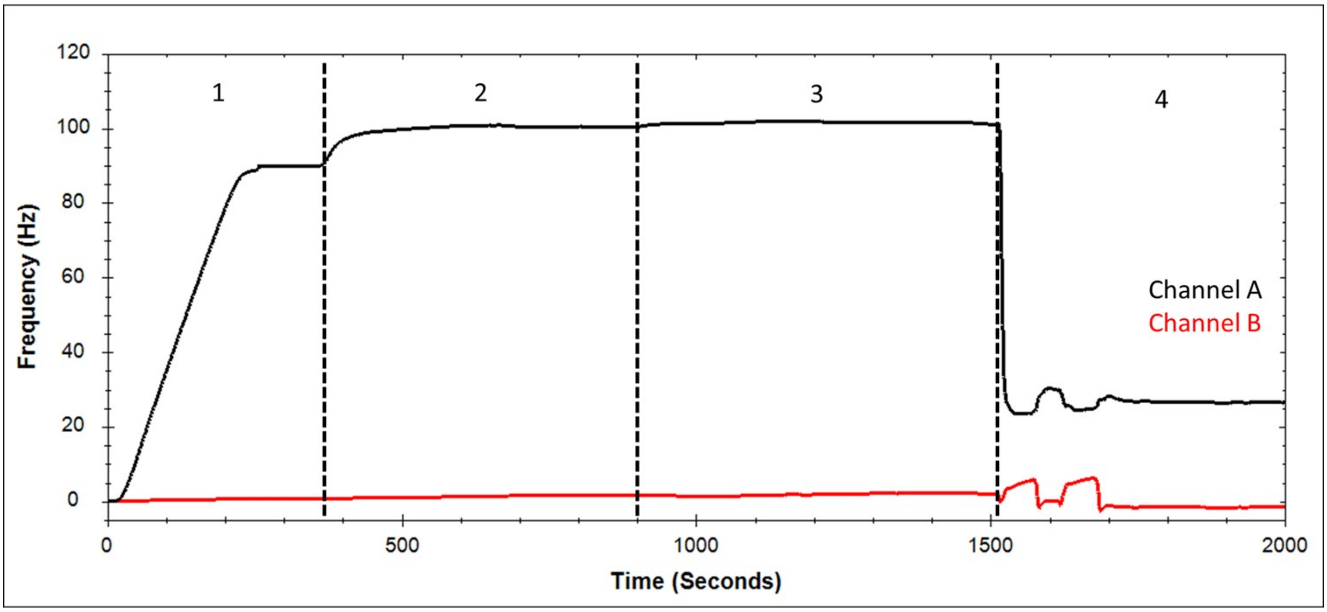

Figure S7. Sensorgram showing: 1) injection of NP solution (channel A), 2,3) two injections of mAb-Tf, employed as secondary antibody (channels A and B), 4) regeneration with two 30 s pulses of 10mM glycine pH 1.5 (channels A and B). Channel A: LNB surface functionalized with mAb-Tf with NPs, Channel B: LNB surface functionalized with mAb-Tf without NPs.

A

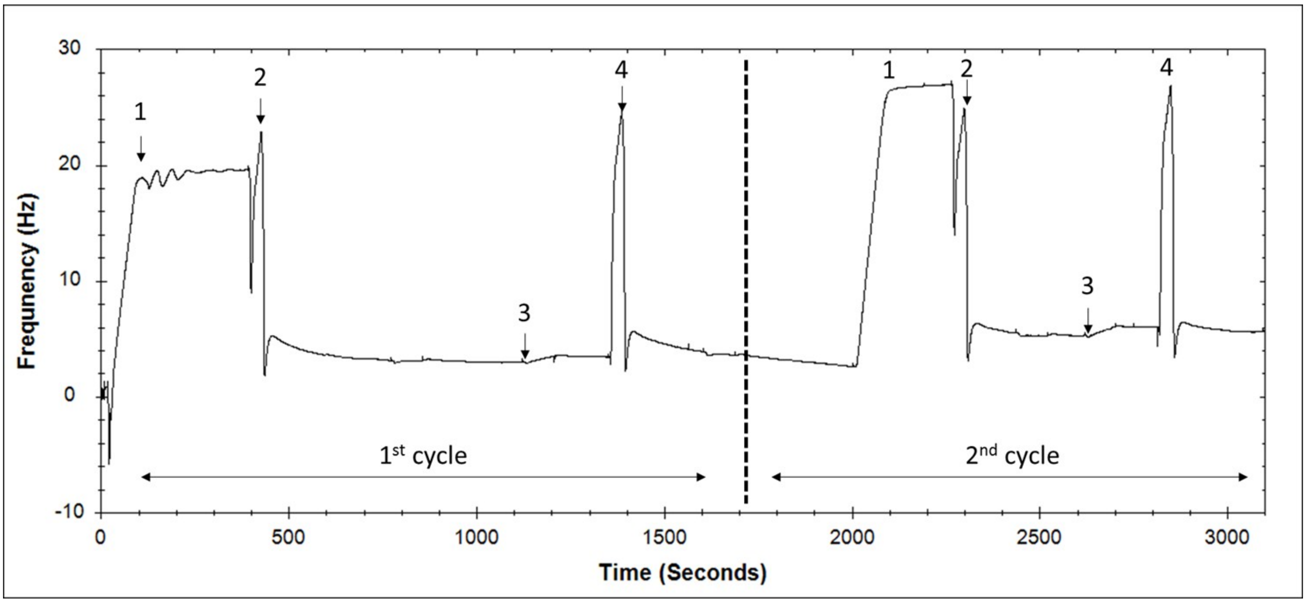

B

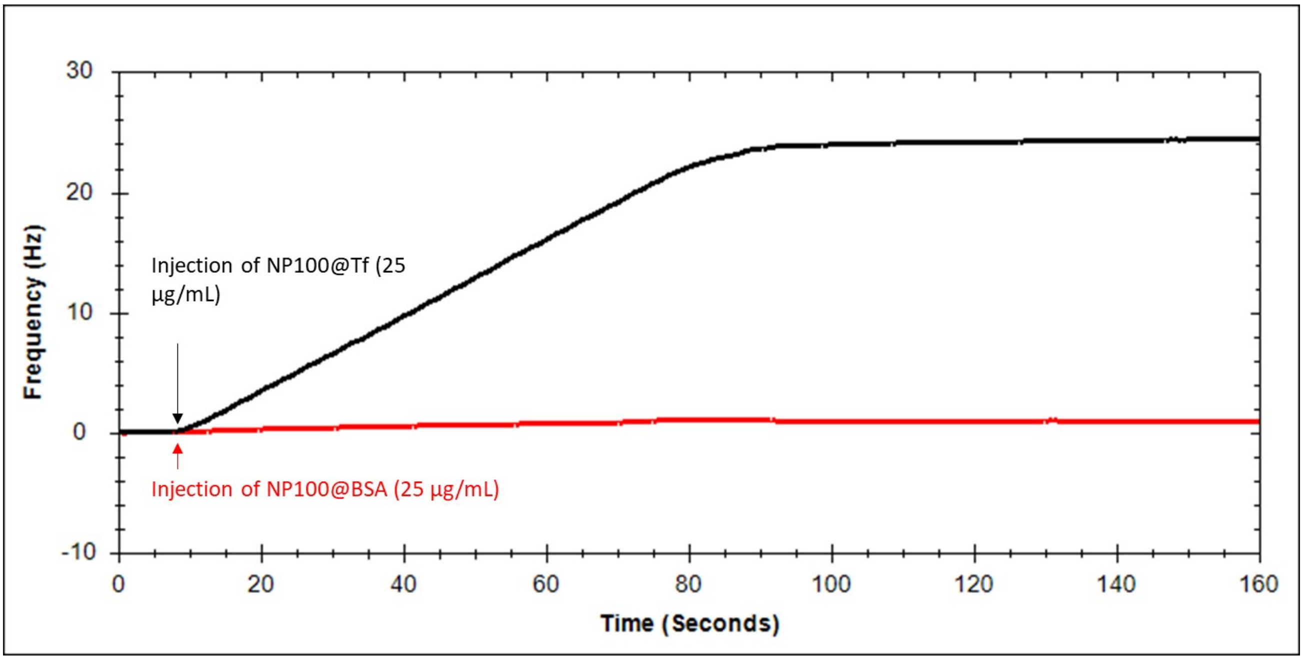

Figure S8. A) Sensorgram showing 1) injection of PS NPs 100 nm incubated with Tf (concentration of 25 µg/mL), followed by 2) regeneration with a 30 s pulse of 10mM glycine pH 1.5, 3) injection of 25 µg/mL of the same particles incubated with BSA (NP@BSA) and 4) another 30 s pulse of glycine regeneration. The experimental cycle was repeated twice. B) Frequency shifts caused by the injection of PS NPs 100 nm incubated with Tf (NP@Tf) (black curve) and by the injection of same particles incubated with BSA (NP@BSA). No binding was observed for particles incubated with BSA (frequency shift zero).

A

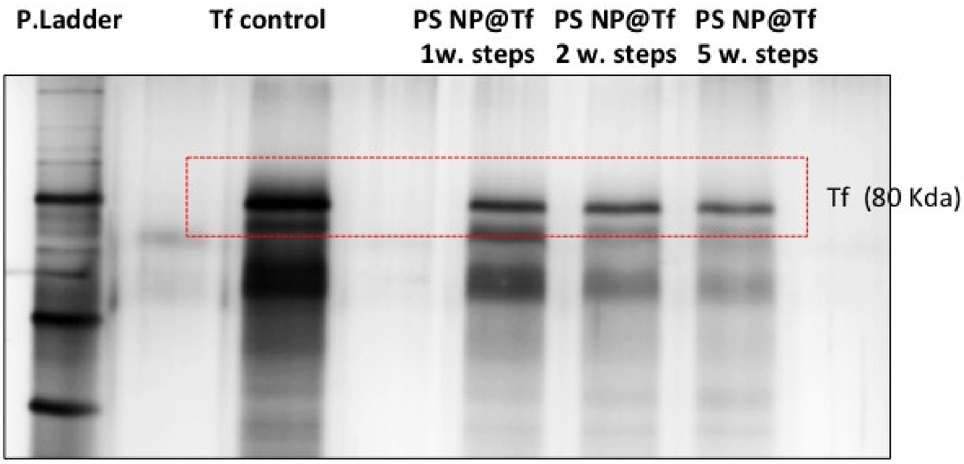

B

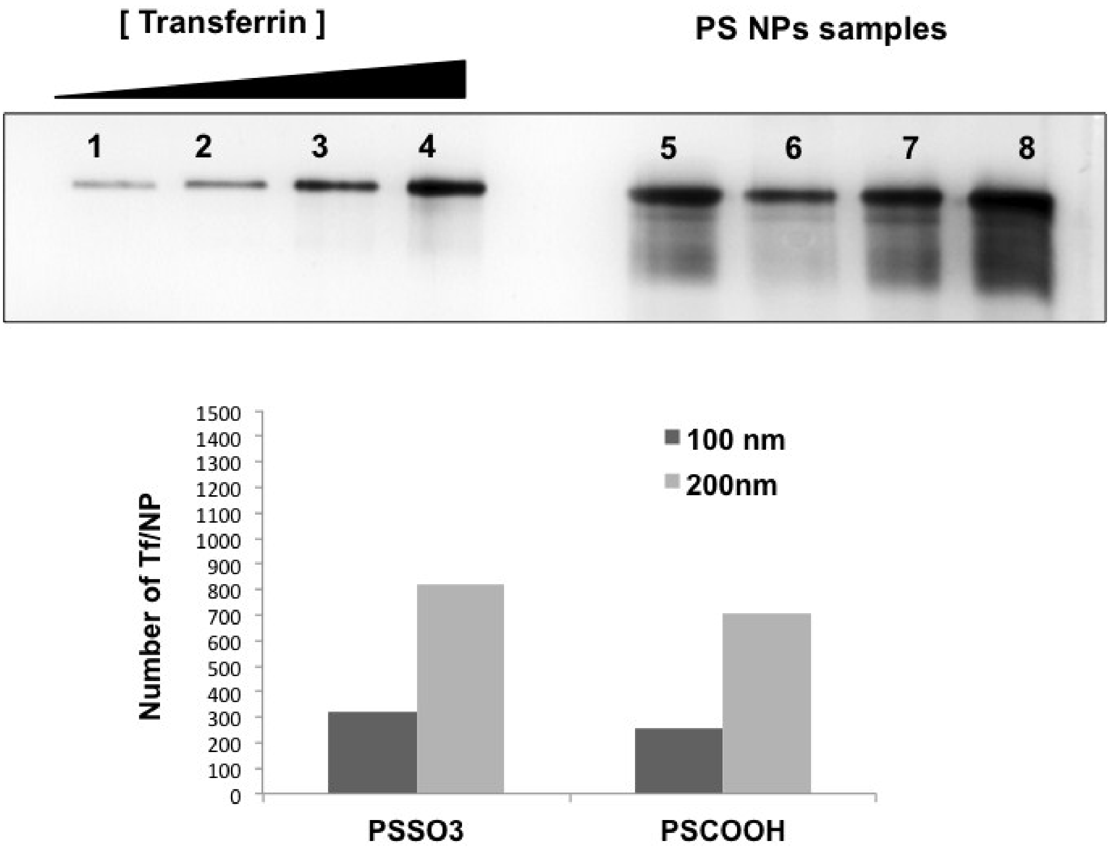

Figure S9. A) SDS-PAGE analysis of the protein hard corona formed onto 200 nm $PSSO_3$ NPs after different washing steps. B) SDS-PAGE images for analysis of Tf adsorbed on the PS@Tf NP complexes.

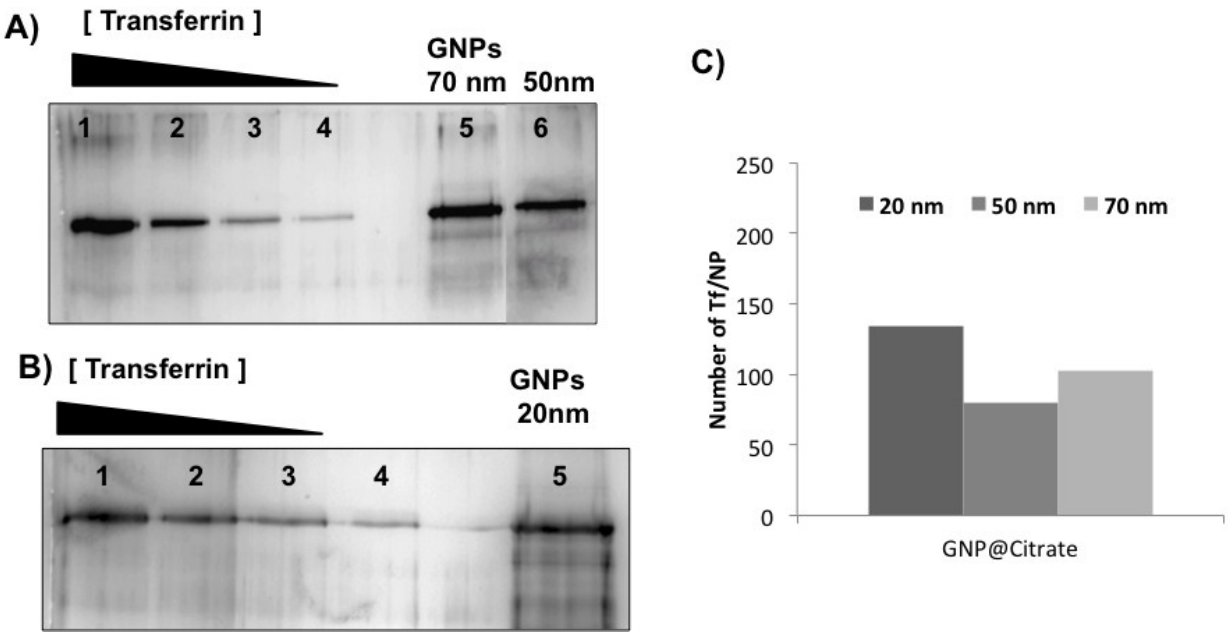

Figure S10. SDS-PAGE images for analysis of Tf adsorbed on the GNP@Tf NP complexes: A) 70 nm and 50 nm GNP@Citrate. B) 20 nm GNP@Citrate.

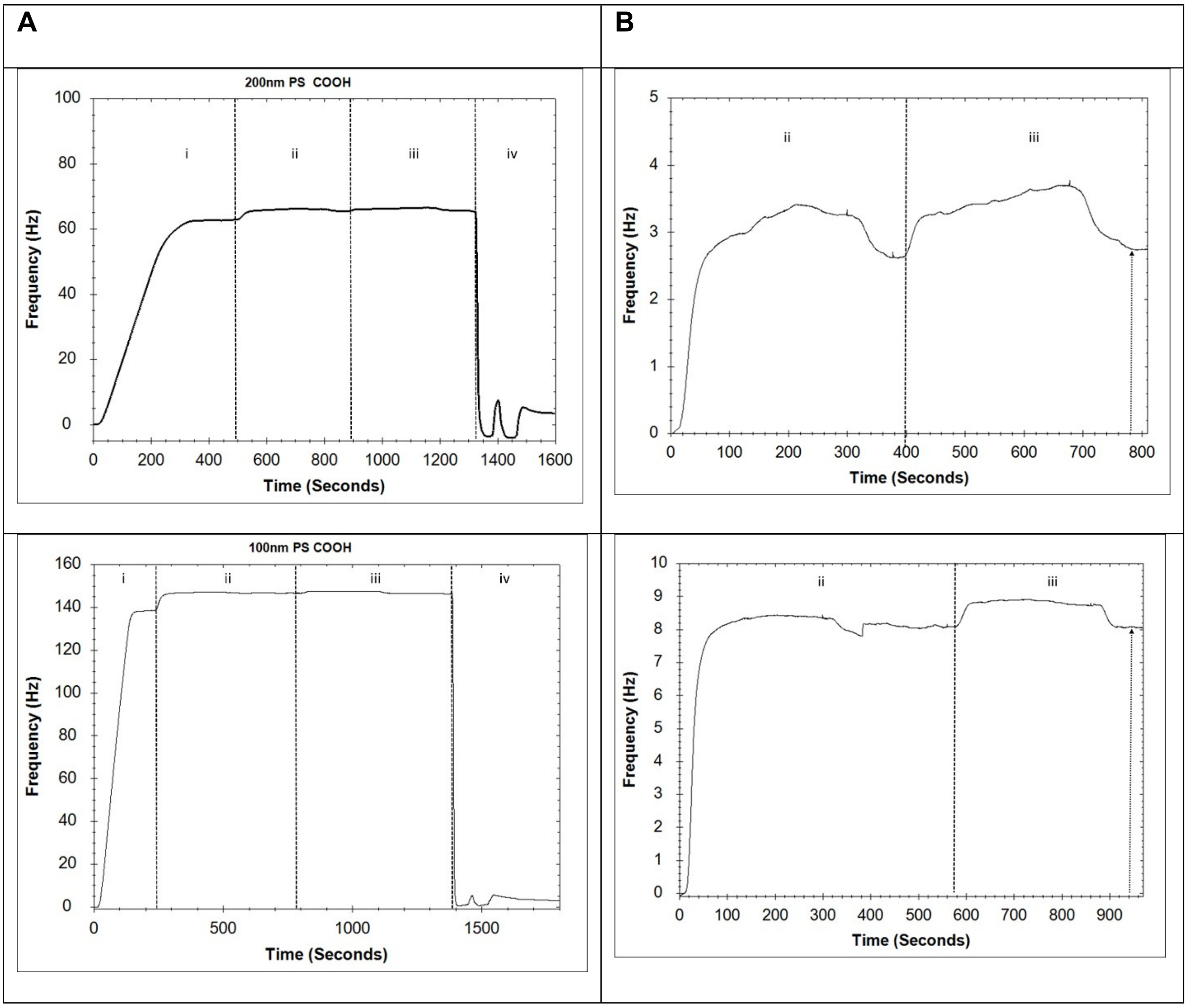

Figure S11. Data from QCM (PS NPs). PS COOH NPs; A) Sensorgrams showing one or multiple injections of NP-Tf complexes (i) followed by subsequent injections (ii, iii) of mAb-Tf until saturation of the surface of the nanoparticle complexes and (iv) regeneration with injection of 10 mM glycine pH 1.5. B) Close-up of the two consecutive injections (ii, iii) of the mAb-Tf.

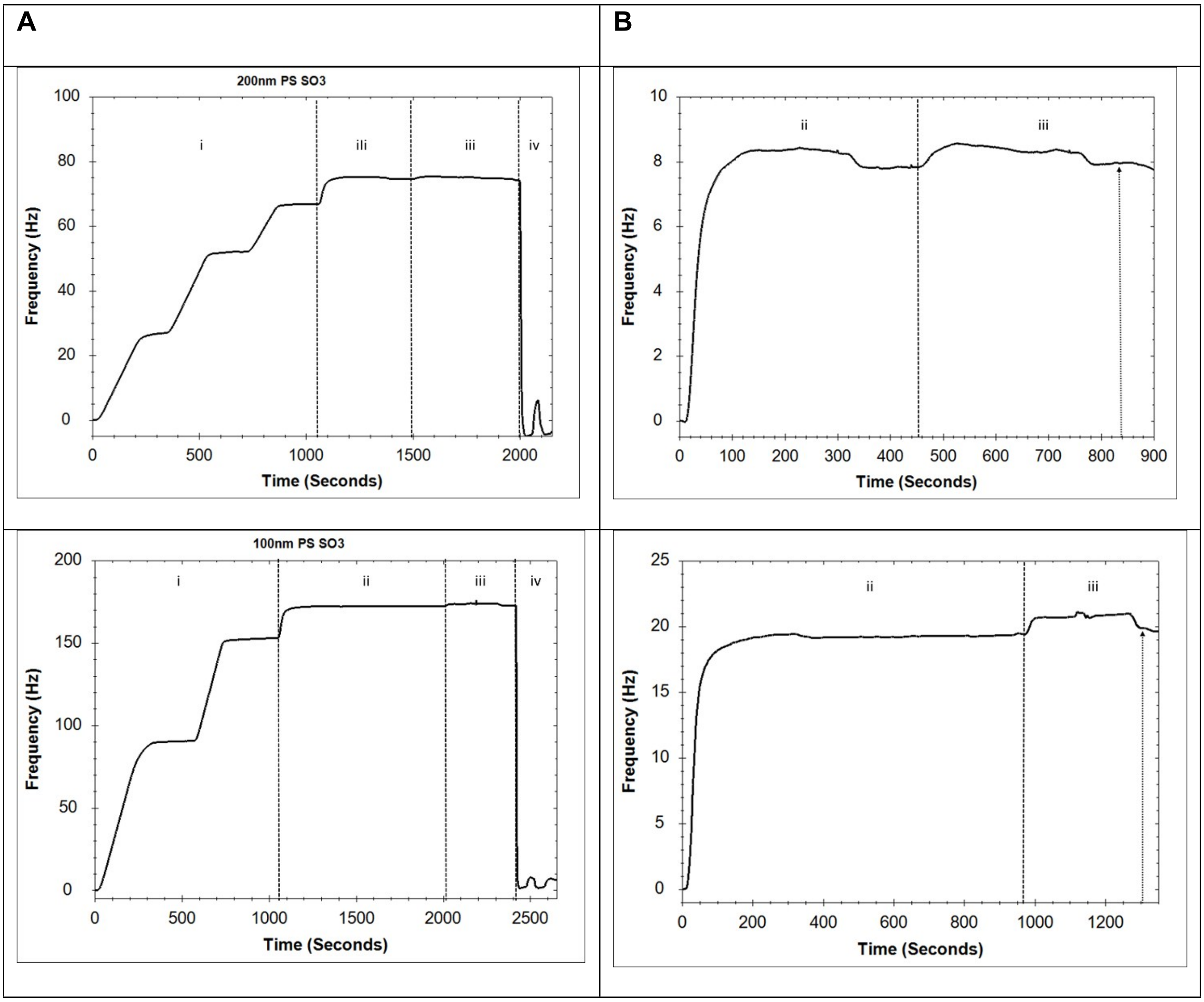

Figure S12. Data from QCM (PS NPs). PS SO3 NPs; A) Sensorgrams showing one or multiple injections of NP-Tf complexes (i) followed by subsequent injections (ii, iii) of mAb-Tf until saturation of the surface of the NP complexes and (iv) regeneration with injection of 10 mM glycine pH 1.5. B) Close-up of the two consecutive injections (ii, iii) of the mAb-Tf

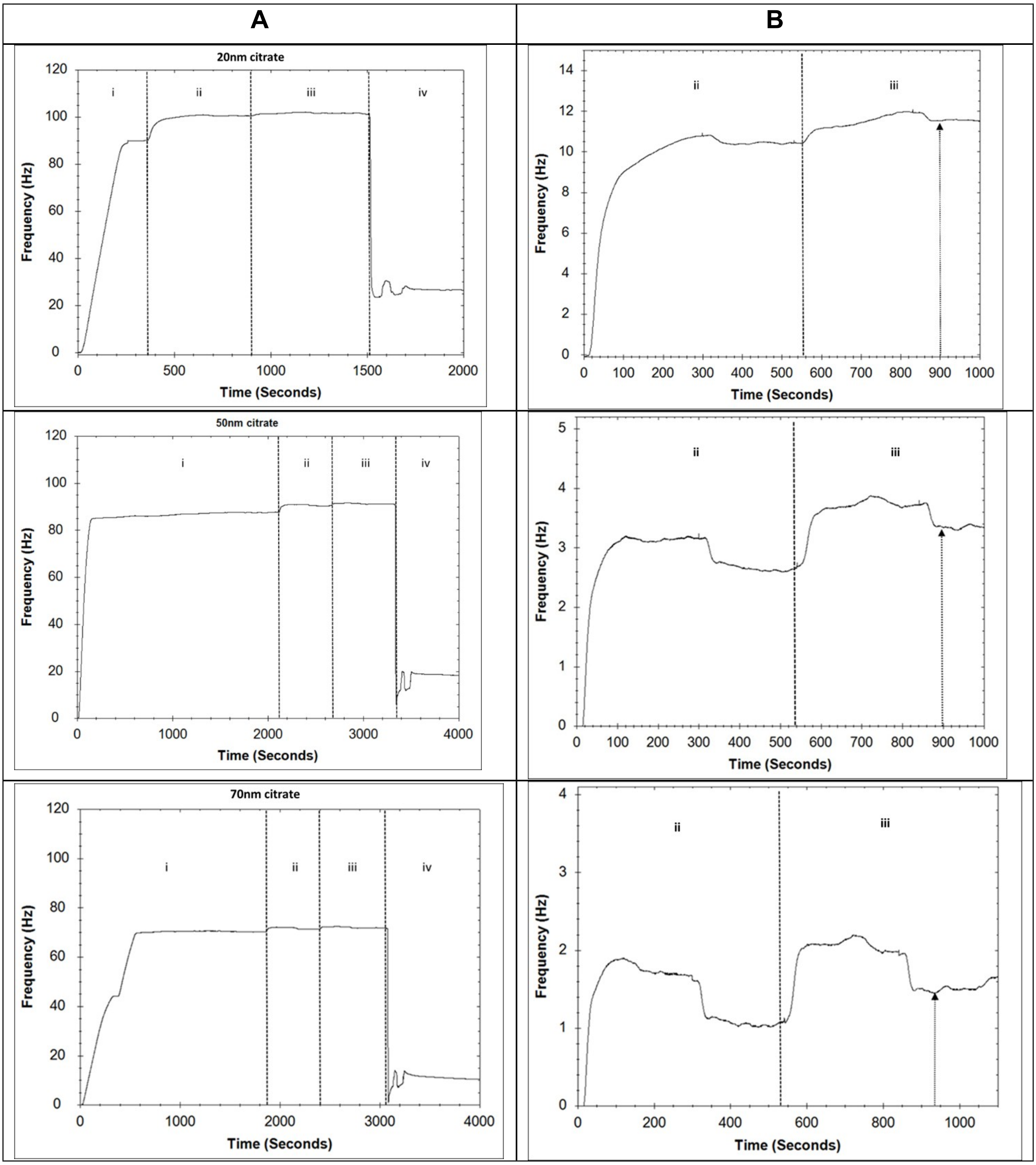

Figure S13. Data from QCM (GOLD Citrate NPs). A) Sensorgrams showing one or multiple injections of nanoparticle complexes (i) followed by subsequent injections (ii, iii) of mAb-Tf until saturation of the surface of the NP-Tf complexes and (iv) regeneration with injection of 10 mM glycine pH 1.5. B) Close-up of the two consecutive injections (ii, iii) of the mAb-Tf.

	PS SO3		PS COOH	
Frequency shift (Hz) mAbc	200	200	200	200
Ab capture mass (ng)	140	140	140	140
Ab capture molecules	5,3E+11	5,3E+11	5,3E+11	5,3E+11
Diameter (nm)	100	200	100	200
Frequency shift (Hz) $_{NPTf}$	**153**	**66,7**	**138,5**	**62,5**
M_{tot} (ng)	107,1	46,69	96,95	43,75
M_{eff} (ng)$_{core\ shell\ model}$	4,53E-08	4,21E-07	5,04E-08	1,83E-07
N of particles immobilized	2,36E+09	1,11E+08	1,92E+09	2,39E+08
area (nm^2)	31416	125664	31416	125664
total nm^2	7,43E+13	1,39E+13	6,04E+13	3,00E+13
Tf per NP (theory)	711	2844	711	2844
Frequency shift (Hz) $_{mAb}$	**20**	**7,75**	**8**	**2,7**
Immobilized ab mass (ng)	14	5,425	5,6	1,89
ab moles	8,75E-14	3,39063E-14	3,5E-14	1,18125E-14
ab molecules	5,27E+10	2,04E+10	2,11E+10	7,11E+09
Number of Abs / particle	22	184	11	30
Abs/nm^2	7,09E-04	1,47E-03	3,49E-04	2,37E-04

Table S3. Summary of data obtained from QCM experiments for PS-Tf NP complexes.

		Au Citrate	
Diameter (nm)	20	50	70
Frequency shift (Hz) $_{particle\ imm}$	**90**	**86**	**70**
M_{tot} (ng)	63	60,2	49
M_{eff} (ng)$_{core\ shell\ model}$	1,175E-07	1,20E-06	3,15E-06
N of particles immobilized	5,36E+08	5,02E+07	1,56E+07
area (nm^2)	1257	7854	15394
total nm^2	6,74E+11	3,94E+11	2,39E+11
Tf per NP (theory)	28	178	348
Frequency shift (Hz) $_{mab\ imm}$	**11,5**	**3,3**	**1,5**
Immobilized ab mass (ng)	8,05	2,31	1,05
ab moles	5,03125E-14	1,44375E-14	6,5625E-15
ab molecules	3,03E+10	8,69E+09	3,95E+09
Number of Abs / particle	57	173	254
Abs/nm^2	4,50E-02	2,21E-02	1,65E-02

Table S4. Summary of data obtained from QCM experiments for GNP-Tf NP complexes.

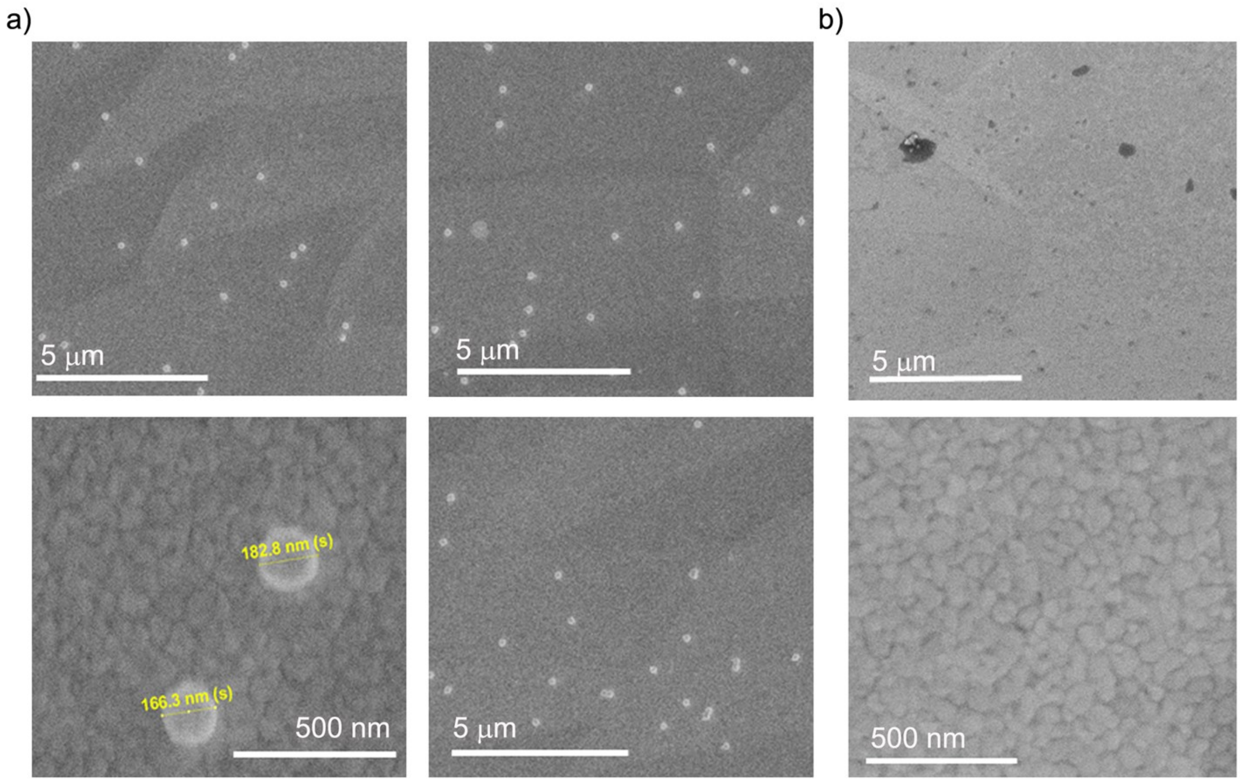

Figure S14. SEM micrographs of chip A (a) functionalized with mAb-Tf after running a solution of 200 nm PS NP incubated with Tf and chip B (b) control.

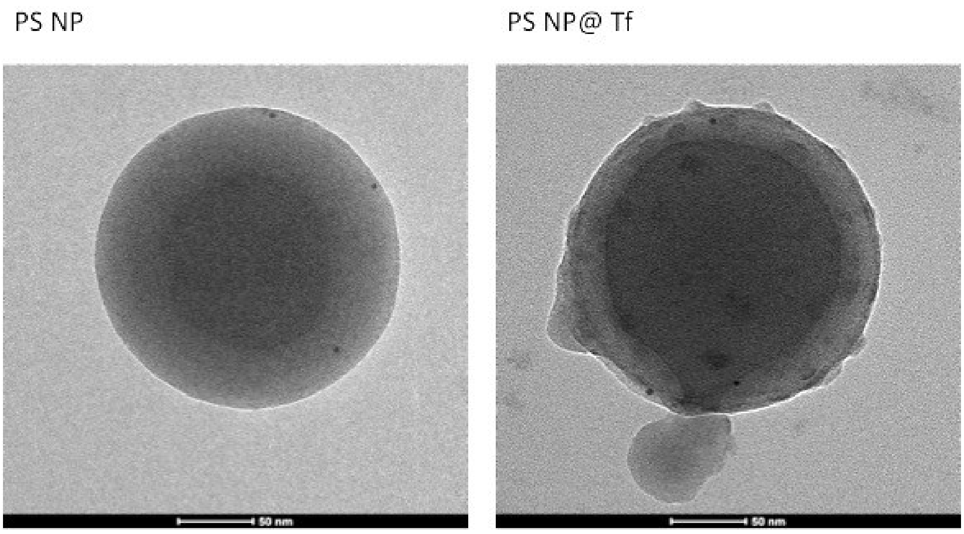

Figure S15. TEM micrographs of 200 nm PS NP with and without Tf coated.

3 References

1. Bastús, N. G.; Comenge, J.; Puntes, V., Kinetically Controlled Seeded Growth Synthesis of Citrate-Stabilized Gold Nanoparticles of up to 200 nm: Size Focusing versus Ostwald Ripening. *Langmuir* **2011,** *27* (17), 11098-11105.
2. Hühn, J.; Carrillo-Carrion, C.; Soliman, M. G.; Pfeiffer, C.; Valdeperez, D.; Masood, A.; Chakraborty, I.; Zhu, L.; Gallego, M.; Yue, Z.; Carril, M.; Feliu, N.; Escudero, A.; Alkilany, A. M.; Pelaz, B.; del Pino, P.; Parak, W. J., Selected Standard Protocols for the Synthesis, Phase Transfer, and Characterization of Inorganic Colloidal Nanoparticles. *Chemistry of Materials* **2017,** *29* (1), 399-461.
3. Sanz, V.; Conde, J.; Hernández, Y.; Baptista, P. V.; Ibarra, M. R.; de la Fuente, J. M., Effect of PEG biofunctional spacers and TAT peptide on dsRNA loading on gold nanoparticles. *Journal of Nanoparticle Research* **2012,** *14* (6), 917.
4. Monopoli, M. P.; Walczyk, D.; Campbell, A.; Elia, G.; Lynch, I.; Baldelli Bombelli, F.; Dawson, K. A., Physical−Chemical Aspects of Protein Corona: Relevance to in Vitro and in Vivo Biological Impacts of Nanoparticles. *Journal of the American Chemical Society* **2011,** *133* (8), 2525-2534.